Journal of Applied Polymer Science

Synthesis and evaluation of fluorosilicone-modified starch for protection of historic stone

Jia Qu,[1,2] Jing Liu,[1] Ling He[1]

[1]Department of Chemistry, School of Science, Xi'an Jiaotong University, Xi'an 710049, China

[2]College of Chemical Engineering and Modern Materials/Shaanxi Key Laboratory of Comprehensive Utilization of Tailings Resources, Shangluo University, Shangluo 726000, China

Correspondence to: H. Ling (e-mail: heling@mail.xjtu.edu.cn)

ABSTRACT: Starch is sensitive to moisture and is weak to durability in the protection application to ancient relics. Therefore, two fluorosilicone-modified starches are firstly prepared and evaluated for the protection of historic stones. The fluoro-silicone copolymer grafted starch of P(VTMS/12FMA)-*g*-starch is synthesized by grafting copolymer of vinyltrimethoxysilane (VTMS) and dodecafluoroheptyl methacrylate (12FMA) onto starch. While the fluoro-silicone starch latex of VTMS-starch@P(MMA/BA/3FMA) is obtained by emulsion polymerization of VTMS primarily grafted-starch (VTMS-starch) with methyl methacrylate (MMA), butyl acrylate (BA) and 2,2,2-trifluoroethyl methacrylate (3FMA). The grafting fluorosilicone copolymer onto starch improves obviously their hydrophobic and thermal properties. Comparatively, VTMS-starch@P(MMA/BA/3FMA) film performs higher water contact angle (107°) and thermal stability (350–430°C) than p(VTMS/12FMA)-*g*-starch film (72°, 250–420°C) due to the migration of fluorine-containing group onto the surface of film during the film formation. Therefore, VTMS-starch@P(MMA/BA/3FMA) shows much better protective performance in water-resistance, and salt/freeze-thaw resistance for stone samples. © 2014 Wiley Periodicals, Inc. J. Appl. Polym. Sci. **2015**, *132*, 41650.

KEYWORDS: ageing; applications; colloids; copolymers; emulsion polymerization

Received 20 June 2014; accepted 13 October 2014

DOI: 10.1002/app.41650

INTRODUCTION

Starch is commonly used in Chinese ancient buildings as the traditional sticky rice–lime mortar,[1] as coating or binding materials,[2] and as repairing material in ancient masonry.[3] Although starch could form isotropic, odorless and colorless film with low-cost and environmental friendly natures, the poor mechanical properties, sensitive to moisture and weaker durability have severely limited the application of starch in protection of ancient relics from the perspective of cultural relics conservation. Therefore, it is necessary to modify starch in order to overcome these disadvantages and to improve the protective application. Unfortunately, there is no any report cared for this purpose up to now. From the point of chemical view, starch is a kind of natural polymer with (1–4)-linked polysaccharide of linear amylose and (1–6)-branched amylopectin. Both amylose and amylopectin are structured by hydrogen bonding. This kind of structure has brought much convenient to the modification of starch by chemical reaction, such as the modification focused at the starch/rubber,[4] starch/ether,[5] and starch/acetate.[6] Actually, grafting polymer onto the starch is an effective way to overcome the disadvantage of pure starch as coating materials.[7]

Considering that the fluoroacrylate grafted-surface could provide with extraordinary surface properties, good thermal and chemical stability and the excellent film-forming property, and the extraordinary adhesion to the substrate through forming covalent bonds provided by acrylic polymers, as well as the generation of low-energy surface by self-segregation and self-organization of -CF_3 groups in the perfluoroalkyl,[8–10] the well-known fluoroacrylate copolymer is expected to be grafted onto starch in this paper to provide the starch with desired surface properties. But one of the most key points is how to introduce the fluorinated acrylic polymers into the hydrocarbon of starch to satisfy the required properties. If the modified starch is used for the protection of historic sandstone, the compatibility between materials and stone substrate is another key point in the conservation field. It lets us consider the silicone-containing materials for excellent hydrophobicity, resistance to high/low temperature, and strong adhesion to the substrate.[11–14] Although the silane coupling agents are commonly used to modify the inorganic oxides,[15,16] there is still some attention given to the modification of OH-bearing substrates by silane coupling agents.[17,18] Furthermore, some researches also show that the silane coupling agents is located at the interface of

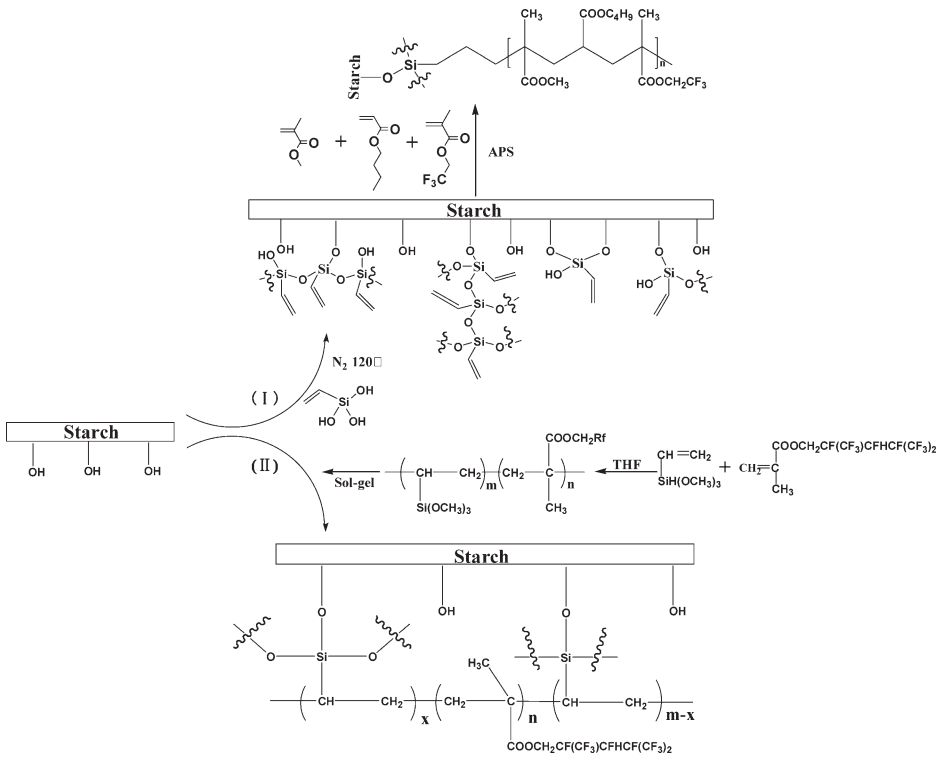

Scheme 1. Synthesis scheme of P(VTMS/12FMA)-*g*-starch (I) and VTMS-starch@P(MMA/BA/3FMA) latex (II).

OH-bearing substrates and copolymer matrix.[19] On the other hand, it has been proved that the previously hydrolysed alkoxysilane could be physically adsorb onto the cellulose fibers at room temperature and then chemically graft after a curing process above 80°C under an inert atmosphere to give a permanent chemical modification of the starch.[20,21]

This article presents the preparation of two fluorosilicone-modified starches and their protective application to the historic stone. The first one is P(VTMS/12FMA)-*g*-starch prepared by free-radical random copolymerization and sol-gel approach via polymer of P(VTMS/12FMA) grafting onto starch. Where, P(VTMS/12FMA) is obtained by dodecafluoroheptyl methacrylate (12FMA) as fluorine-containing monomer and vinyltrimethoxysilane (VTMS) as silicone-containing monomer. The second one is VTMS-starch@P(MMA/BA/3FMA) latex obtained by VTMS primarily grafted onto starch via condensation between Si-OH and C-OH at 120°C, and then P(MMA/BA/3FMA) copolymer by MMA, BA and 2,2,2-trifluoroethyl methacrylate (3FMA) is grafted onto the VTMS-starch by emulsion polymerization. The properties of two fluorosilicone-modified starches are characterized for their chemical structure, morphology in solution, surface wettability of films and the thermostability. Their performances used for the protection of historic stone are evaluated by the color variation, water-resistance, as well as salt and freeze-thaw resistance after protection.

EXPERIMENTAL

Materials

Soluble starch is purchased from Guangdong Guanghua Sci-tech Company, China. It is processed from a kind of potato starch and treated by acid degradation. The molecular weight of purchased starch is about 50,000 g mol^{-1} and the content of amylose is over 90 wt %. 2,2,2-Trifluoroethyl methacrylate (3FMA, $H_2C=C(CH_3)CO_2CH_2CF_3$, 99 wt %) and dodecafluoroheptyl methacrylate (12FMA, $H_2C=C(CH_3)COOCH_2CF(CF_3)CHF\ CF(CF_3)CF_3$, 99 wt %) are supplied by Xuejia Company of China. Methyl methacrylate (MMA, 99 wt %) and butyl acrylate (BA, 99 wt %) are supplied by Aldrich, which are rinsed with 5 wt % NaOH aqueous solution and deionized water until the rinsed water reached pH = 7 before using. Vinyltrimethoxysilane (VTMS, $H_2C=CHSi(OCH_3)_3$, >96 wt %), gained from Silicone New Material Company of Wuhan University (China), is dried with CaH_2 overnight and distilled under reduced pressure. Ammonium persulfate (APS), alkylphenol ethoxylates (OP-10), sodium dodecyl sulfate (SDS), perfluorooctanesulphonate (PFOS), benzoyl peroxide (BPO), hydrochloric acid (HCl), methanol (CH_3OH) and tetrahydrofuran (THF) in analytical purity are purchased commercially and are used as received without further purification.

Preparation of P(VTMS/12FMA)-g-Starch

P(VTMS/12FMA)-*g*-starch is prepared by free-radical random copolymerization and sol-gel approaches as Scheme 1(I). The first step is to synthesize fluorosilicone copolymer P(VTMS/12FMA) using VTMS and 12FMA as follows. After 12FMA and VTMS are dissolved in THF solvent in a three-neck flask connecting a condenser and thermometer with stirring, BPO initiator is added as the molar ratio of 12FMA:VTMS:THF:BPO = 1 : 1 : 60 : 0.01.[22] The reaction is permitted to last for 3 h at 65°C. After the concentrated colorless solution is reprecipitated into methanol and dried in a vacuum oven overnight, the fluorosilicone copolymer of P(VTMS/12FMA) is obtained.

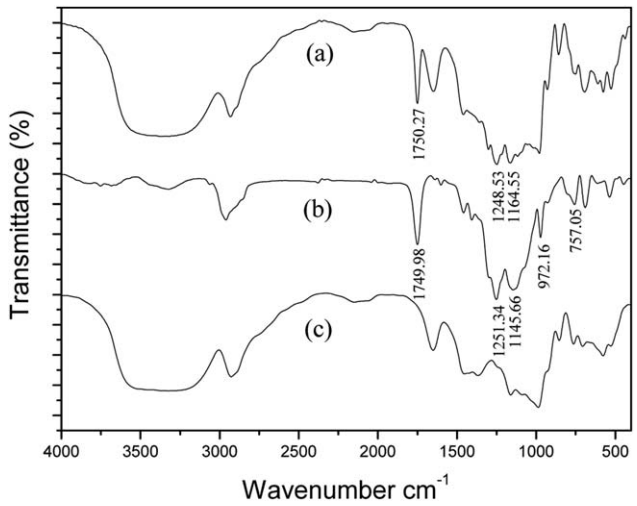

Figure 1. FTIR spectra of P(VTMS/12FMA)-*g*-starch (a), P(VTMS/12FMA) (b), and starch (c).

The second step is grafting P(VTMS/12FMA) onto starch. When P(VTMS/12FMA) is prehydrolyzed in THF in a three-neck flask, using HCl as acidic catalyst to adjust pH to 3, and a 5% (w/w) starch suspension is prepared in THF, the grafting reaction is allowed by adding the prehydrolyzed P(VTMS/12FMA) into the prepared starch suspension. After being stirred at 60°C for 12 h in a water bath, the obtained suspension liquid is centrifuged, and the sediment in the bottom is dried. Then Soxhlete extract the sediment in THF for 6 h to remove the nongrafted P(VTMS/12FMA).

Preparation of VTMS-Starch@P(MMA/BA/3FMA) Latex

VTMS-starch@P(MMA/BA/3FMA) latex is obtained by physical adsorption and chemical grafting as Scheme 1(II). Firstly, the suspension of starch in a mixture of ethanol/water = 80/20 (v/v) and the prehydrolyzed VTMS in water/VTMS = 1/1 (molar ratio) are prepared at room temperature for 2 h, separately. Then, the prehydrolyzed VTMS is adsorbed onto starch suspension by stirring at pH = 4 for 2 h. The VTMS-adsorbed starch is centrifuged at 2500 rpm for 20 min, vacuum dried at room temperature to remove water and alcohol, and then heated at 120°C under a nitrogen atmosphere for 2 h. After the cured starch is extracted in THF for 24 h in order to remove the nongrafted VTMS, the VTMS chemically grafted starch (VTMS-starch) is obtained.

Then, VTMS-starch (5 wt %) is gelatinized in water at 85°C for 30 min by the help of a mixed emulsifier of OP-10/SDS/PFOS in the ration of 3.3/1.67/0.1 (w/w) in a four-mouth-flask equipped with thermometer, stirrer and reflux condenser. $NaHCO_3$ and APS are added into the flask successively after the gelatinized starch is cooled to 70°C in the water bath. The mixture of MMA, BA, and 3FMA in MMA/BA/3FMA = 3/4/3 (w/w) is slowly dripped within 4 h according to the previous research.[21] VTMS-starch@P(MMA/BA/3FMA) latex is obtained after the copolymerization is kept for 1 h at 75°C in the weight ratio of VTMS-starch to P(MMA/BA/3FMA) = 1 : 3.

Characterization of Modified Starch

The chemical structure of P(VTMS/12FMA)-*g*-starch is characterized using a Tensor 27 FTIR spectrometer of BRUKER OPTICS in the recordation with a resolution of 4 cm^{-1}. Background scans are obtained using the KBr powder. VTMS-starch@P(MMA/BA/3FMA) latex (after washing off the copolymer of p(MMA/BA/3FMA) in the latex) is proved by X-Ray photoelectron spectroscopy (XPS) measurement processed on the powder by an AXIS ULTRA (England, KRATOS ANALYTICAL Ltd) using an Al-Ka monochromatic X-ray source (1486.6 eV) operated at 150 W. The overview scans are obtained in energy of 160 eV and acquisition time of 220 s.

The morphology of modified starch in solution is observed with a JEM-200CX transmission electron microscope (TEM) at an acceleration voltage of 120 kV. Their aggregates are detected using a MALVERN Nano ZS 90 (Malvern Instruments, UK) dynamic light scattering (DLS) equipped with a He–Ne laser recorded at 25 ± 0.1°C and at a scattering angle of $2\theta = 173°$.

The films are prepared by dropping the solution of P(VTMS/12FMA)-*g*-starch in hot water or VTMS-starch@P(MMA/BA/3FMA) latex onto the glass slides at ambient temperature for 72 h. The wettability of films is investigated by the static contact angles (SCAs) for both deionized water and hexadecane on the air-exposed film surfaces, which is performed on a JY-82 contact angle goniometer (Hebei Chengde Testing Machine Co. Ltd China) by the sessile drop method with a microsyringe at 25°C. An average of nine readings of contact angles is used as the final value for each sample. The surface free energy of film surfaces is evaluated by applying the Owens and Wendt method. The thermal decomposition of samples is obtained using thermogravimetric analysis (TGA), carried out in a nitrogen atmosphere using a NETZSCH TG209 apparatus by heating the sample from 25 to 600°C with a heating rate of 20°C per minute.

Protection of Historic Stone

The historic stone samples are collected from DaFoSi Grotto of Shaanxi province, a famous Great Buddha Grotto in China. The stone samples are cut into 5 × 5 × 2 cm^3 approximately, washed with deionized water, dried at 105°C up to constant weight (24 h), and then stored in silica gel desiccators before treatment.

The protective treatment on stone samples is performed by capillary absorption from a filter paper pad saturated with modified starch. The treated stone samples are kept a 4-week interval under 55% R.H before starting the final examination so as to allow it penetrated deeply.

The measurements of water absorption are conducted by using the gravimetric method according to total completely immersion. The color variation of stone surface is evaluated by colorimetric measurements using a Konica Minolta Colorimeter (CR-400).[23,24] Water capillary absorption is performed according to the Italian Standard UNI 10859.[25,26] The capillary absorption coefficient is calculated at the end of the test for all the samples.[27] The results refer to average values for three samples.

Water vapor permeability (expressed as g cm^{-2} day^{-1}) indicates the amount of water permeated through the surface of the stone in 1 day (24 h). The water vapor permeability test is processed as follows[28]: using a plasticine and wax to seal the top of the cylinder sandstone samples (4.0 × 0.8 cm^2), and then put it

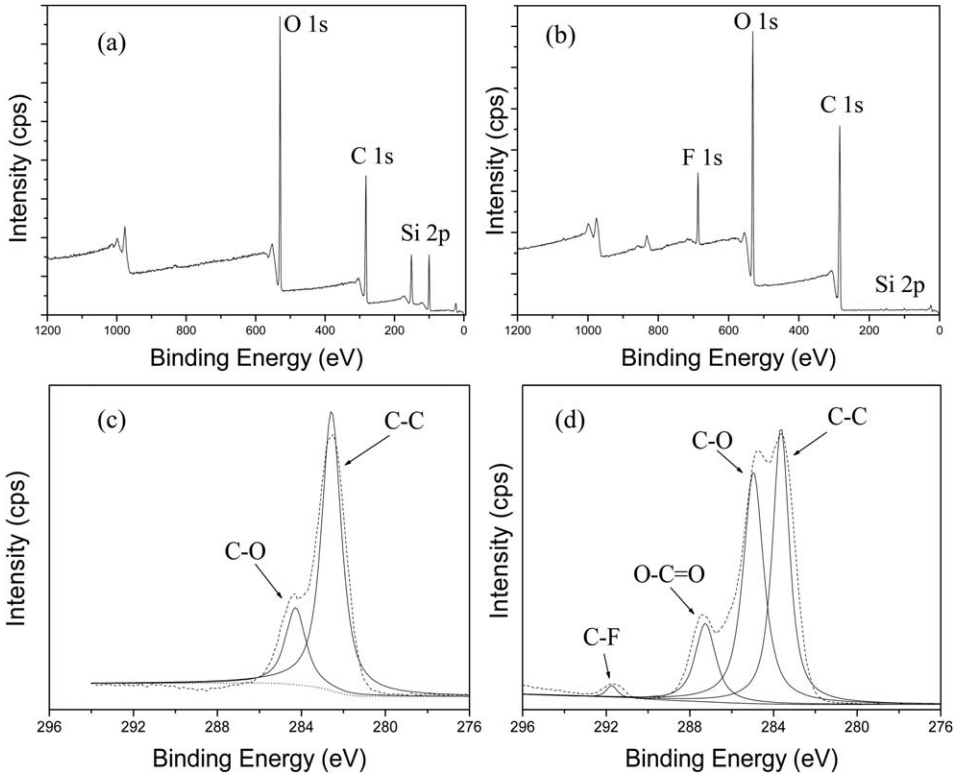

Figure 2. Low-/high-resolution XPS patterns of VTMS-starch (a,c) and VTMS-starch@p(MMA/BA/3FMA) latex extracted by $CHCl_3$ (b,d).

into a beaker partially filled with water, making sure that the vapor could only traverse through the bottom of stone cylinder. Then the above-mentioned system is moved to a desiccator, and kept at a vacuum degree of −0.09 MPa and at constant temperature of 30°C.

The anti-salt and anti-freeze/thaw decay behavior of stone samples are processed as follows[29–31]: (i) total immersion into a saturated solution of Na_2SO_4 for 24 h and (ii) drying at 105∼110°C for 24 h. This cycle is repeated until obvious damage appeared. The freeze-thaw cycle is done as follows: (i) total immersion in deionized water at 20∼25°C for 4 h and (ii) freezing at −4°C for 4 h. This cycle is repeated up to twenty times. The weight loss percentage of the samples (measured at the end of cycle) is taken as a measure of the damage.

The ultraviolet ageing is conducted at room temperature and relative humidity of 50% using a Q8 accelerated aging test chamber equipped with a UVB-313 lamp.[32]

RESULTS AND DISCUSSION

Chemical Structure of Two Fluorosilicone-Modified Starch

Figure 1 is FTIR spectra of P(VTMS/12FMA)-*g*-starch (a), P(VTMS/12FMA) copolymer (b) and starch (c). In order to confirm the formation of P(VTMS/12FMA) copolymer, Figure 1(b) is recognized to find the typical absorption peaks at 1749.98 cm^{-1} for stretching vibration of C=O in the –COO– in MMA, 1251.34 cm^{-1} for the stretching vibration of $–CF_3$ and –CF– in 12FMA, 1145.66 cm^{-1} for antisymmetric stretching vibration of –Si–O–C groups, 972.16 cm^{-1} for the stretching vibration of –C–O–, and 757.05 cm^{-1} for wagging vibration of $–(CH_2)_n$ $(n>4)$, but it is not observed the stretching vibration of C=C groups at 1600–1680 cm^{-1}, which indicates that the polymerization of VTMS and 12FMA has formed C–C backbone in P(VTMS/12FMA) copolymer. Then, the comparison of Figure 1(a) with Figure 1(b,c) shows that 1750.27 cm^{-1} for –COO–, 1248.53 cm^{-1} for $–CF_3$ and –CF–, 1164.55 cm^{-1} for –Si–O–Si and –Si–O–C reveals the grafting of P(VTMS/12FMA) onto the starch, especially 1164.55 cm^{-1} for –Si–O–Si and –Si–O–C indicating the possibility of hydrolysis reaction of the introduced starch (-O-H bond) with $-Si(OCH_3)_3$ bond in P(VTMS/12FMA) copolymer.

Since FTIR spectra is lack to confirm the formation of VTMS-starch@P(MMA/BA/3FMA) latex, the XPS patterns of VTMS-starch (the nongrafted VTMS has been washed off by THF) and VTMS-starch@P(MMA/BA/3FMA) extracted by $CHCl_3$ are used to prove the formation of latex (Figure 2). The low-resolution XPS patterns for VTMS-starch in Figure 2(a) could confirm that the VTMS has been chemical grafted onto the starch by the presence of silicon atoms witnessed at the corresponding peaks of 100 and 150 eV. The XPS pattern for extracted latex by $CHCl_3$ in Figure 2(b) clearly reveals the presence of fluorine and silicon atoms, which confirms the formation of VTMS-starch@P(MMA/BA/3FMA) latex. For

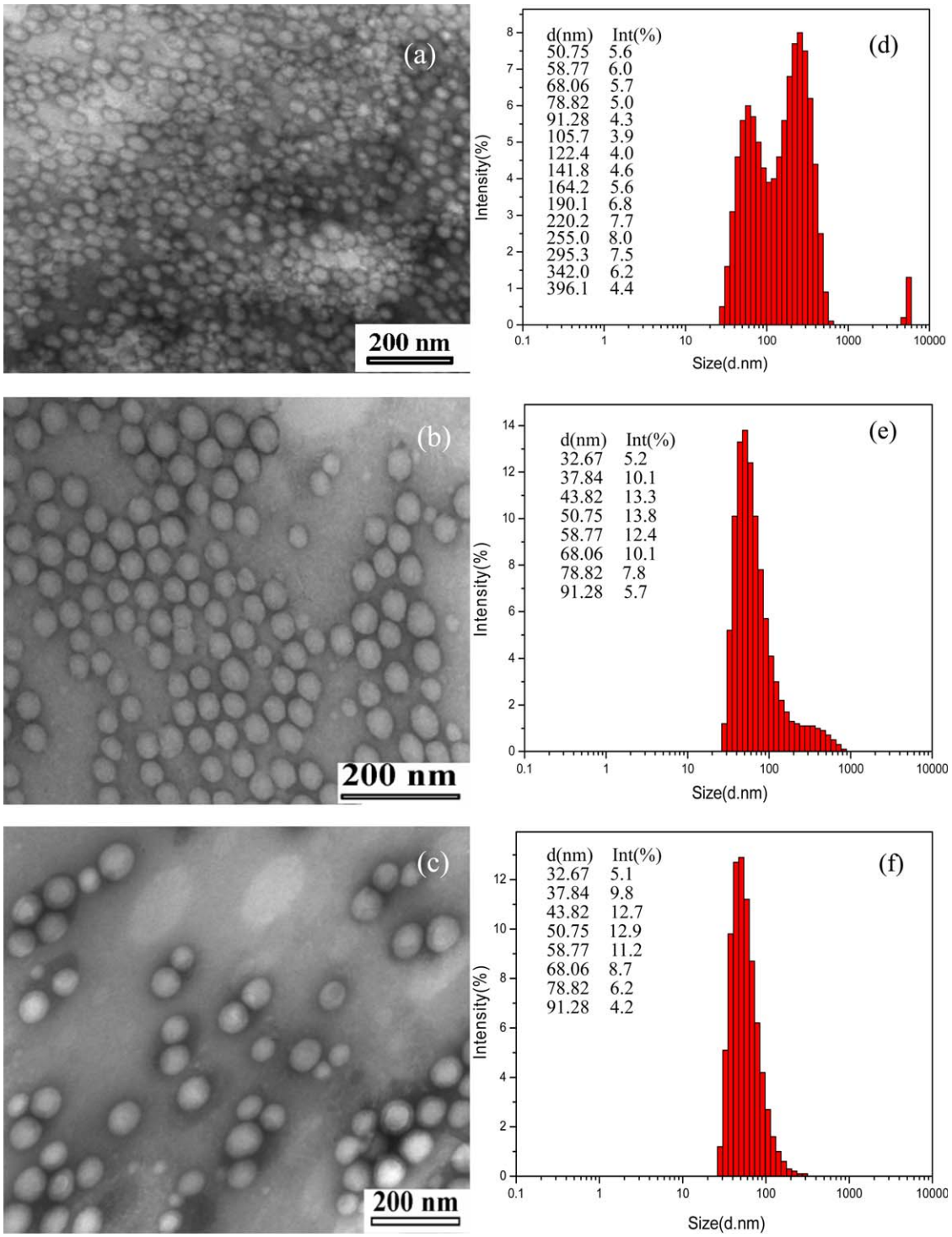

Figure 3. TEM images and DLS curves of starch (a,d), P(VTMS/12FMA)-*g*-starch (b,e), and VTMS-starch@P(MMA/BA/3FMA) (c,f). [Color figure can be viewed in the online issue, which is available at wileyonlinelibrary.com.]

the high-resolution XPS patterns of VTMS-starch [Figure 2(c)] and VTMS-starch@P(MMA/BA/3FMA) latex after extraction [Figure 2(d)], the groups of C-O, O-C=O and C-F could further confirm the synthesis of VTMS-starch@P(MMA/BA/3FMA).

The Surface Wettability of Films

Because the aggregates in solution of fluorosilicone-modified starches contribute much to the film properties and the protective performances, their morphologies and aggregated size distributions are determined by TEM and DLS. Starch is used for

Table I. Size Distribution, Static Contact Angles and Surface Free Energy of Films

Sample	Size distribution		θ_w(°)	θ_h(°)	γ_s (mN/m)
	TEM (nm)	DLS (nm)			
Pure starch	40	50–300	51	0	51.32
P(VTMS/12FMA)-*g*-starch	40–60	40–90	72	32	35.80
VTMS-starch@P(MMA/BA/3FMA)	60–80	40–90	107	25	25.19

the comparison. Due to the interaction of C-OH in the starch making different size of aggregation, a very wide particles distribution of 50–300 nm for the starch [Figure 3(a,d)] is found. But after modification, the narrow particles size distribution as 40–90 nm (Table I) is obtained for P(VTMS/12FMA)-*g*-starch [Figure 3(b)] and VTMS-starch@P(MMA/BA/3FMA) [Figure 3(c)], which is attributed to chemical modification to prevent the modified starch from aggregation into larger size. Therefore, the particles size distribution in Figure 3(e) for P(VTMS/12FMA)-*g*-starch and Figure 3(f) for VTMS-starch@P(MMA/BA/3FMA) becomes much narrow.

Actually, the photograph of two fluorosilicone-modified starch films for visual understanding in Figure 4 shows translucent and continuous features. Table I gives the results of static contact angles (SCAs) for both deionized water and hexadecane on the air-exposed film surfaces, and the calculated surface free energy of films. It is clear to see that the contact angles of modified starch films are increased obviously compared with pure starch film (51° for water), indicating the hydrophobic/oleophobic property of modified films. Comparatively, the film from VTMS-starch@P(MMA/BA/3FMA) latex performs higher

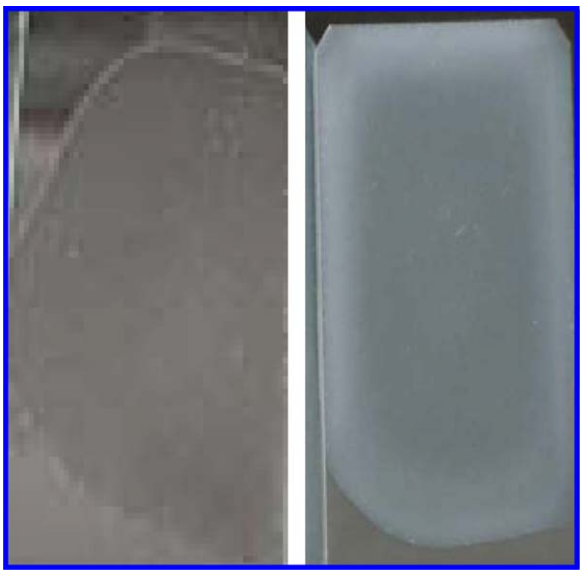

Figure 4. The photograph of P(VTMS/12FMA)-*g*-starch film (left) and VTMS-starch@P(MMA/BA/3FMA) film (right). [Color figure can be viewed in the online issue, which is available at wileyonlinelibrary.com.]

Table II. XPS Analysis of Film Surfaces and Powders

Samples	Atomic composition (%)			
	F	Si	O	C
P(VTMS/12FMA)-*g*-starch film surface	43.69	0.52	11.61	44.18
P(VTMS/12FMA)-*g*-starch powder	8.24	3.84	26.82	61.10
VTMS-starch@p(MMA/BA/3FMA) film surface	28.76	0.41	22.77	48.06
VTMS-starch@p(MMA/BA/3FMA) powder	5.38	0.69	27.60	66.34

water contact angle (107°) but a little lower hexadecane contact angle (25°) than P(VTMS/12FMA)-*g*-starch film (72, 32°), which lends to its much lower surface free energy of films (25.91 m*N*/m) than P(VTMS/12FMA)-*g*-starch film (35.80 m*N*/m). Furthermore, the starch film gives 45% water absorption, but the films form modified starch give almost no water absorption, showing the modified films excellent water resistance.

In order to understand how the fluorosilicone-modified starches form this kind of film, the XPS analysis of film surfaces and the powder of obtained fluorosilicone-modified starch is conducted. The elemental composition from XPS analysis in Table II indicates that, during the film formation, the fluorine-containing group could migrate onto the surface of film to improving the F content, such as 43.69% in film surface but 8.24% in the powder for P(VTMS/12FMA)-*g*-starch, and 28.76% in film surface and 5.38% in the powder for VTMS-starch@p(MMA/BA/3FMA). While, the silicon-containing group on the surface of film is reduced from 3.84% on the film surface to 0.52% in the powder for P(VTMS/12FMA)-*g*-starch, and from 0.69% on the

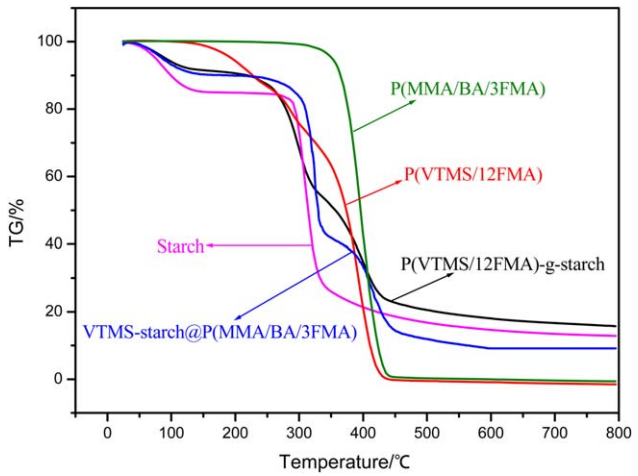

Figure 5. TGA curves of starch, P(VTMS/12FMA), P(MMA/BA/3FMA), P(VTMS/12FMA)-*g*-starch, and VTMS-starch@P(MMA/BA/3FMA). [Color figure can be viewed in the online issue, which is available at wileyonlinelibrary.com.]

Table III. The Color Variation of Stone Specimens After Protection

Protective material	ΔL	Δa	Δb	ΔE
Starch	−0.23	1.13	2.18	2.48
P(VTMS/12FMA)-*g*-starch	−1.58	1.20	1.90	2.80
VTMS-starch@p(MMA/BA/3FMA)	−0.51	1.46	2.75	3.16

film surface to 0.41% in the mitrax for VTMS-starch@p(MMA/BA/3FMA). Actually, this migration of fluorine-containing group onto the surface of film for two fluorosilicone-modified starches during the film formation is similar in increase of F content compared with the powder, 5.302 times for P(VTMS/12FMA)-*g*-starch and 5.346 times for VTMS-starch@p(MMA/BA/3FMA). Therefore, this enrichment of fluorine-containing groups on the film surface could lower the surface free energy for the surface hydrophobicity, such as the film from VTMS-starch@P(MMA/BA/3FMA) latex performs higher water contact angle (107°) than P(VTMS/12FMA)-*g*-starch film (72°).

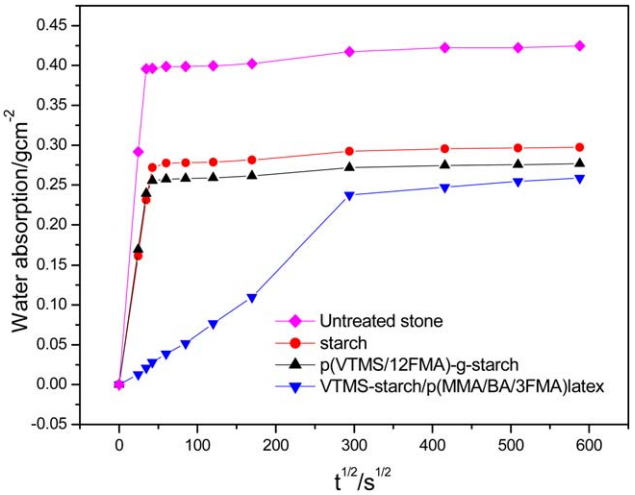

Figure 6. Capillary absorption curves for untreated and treated samples. [Color figure can be viewed in the online issue, which is available at wileyonlinelibrary.com.]

The Thermal Stability of Fluorosilicone-Modified Starch

The thermal stabilities of both films are further investigated by TGA with the thermal degradability in the range of 25–800°C under nitrogen atmosphere, as shown in Figure 5. Comparing with starch with a sharp drop at 290–320°C to show the thermal decomposition, the copolymer film of P(VTMS/12FMA) starts to decompose at 150°C and decomposes totally at 420°C, but P(VTMS/12FMA)-*g*-starch performs a drop at 250–420°C (250–290°C for starch and from 320 to 420°C for P(VTMS/12FMA)). The weightlessness peak becomes wide due to the graft of P(VTMS/12FMA). Furthermore, compared with the pure starch, the modified starch of P(VTMS/12FMA)-*g*-starch shows lower sensitivity to moisture under 100–120°C from 16% mass loss for starch and about 8.3% for P(VTMS/12FMA)-*g*-starch due to the evaporation of free water adsorption.

For the thermal degradation curve of P(MMA/BA/3FMA), only one step of decomposition starting at 350°C and decomposes totally at 430°C is obtained. While, the degradation process of VTMS-starch@p(MMA/BA/3FMA) is composed of three steps. The first step starts from room temperature to 120°C with the weight loss about 9.1% due to the evaporation of absorbed water, the second step from 300 to 320°C is due to the decomposition of starch, and the third step from 320 to 430°C slows down with a new degradation process of VTMS-starch@p(MMA/BA/3FMA). Comparatively, although both P(VTMS/12FMA)-*g*-starch and VTMS-starch@p(MMA/BA/3FMA) demonstrate the good compatibility between their components, VTMS-starch@p(MMA/BA/3FMA) could provide with better thermal stability (350–430°C) than P(VTMS/12FMA)-*g*-starch (250–420°C).

The Evaluation of Protective Performance to Historic Stone

In order to understand the protective performance of fluorosilicone-modified starches to historic stone, the color variation, water-resistance, water vapor permeability, the ultraviolet ageing, as well as salt and freeze-thaw resistance after protection are evaluated. Table III shows the color variation of stone samples after protection. L values present the brightness, while the values of *a* and *b* refer to the red-green and yellow-blue color, respectively. The value of ΔE represents the color variation between the treated and the untreated stone surfaces, which is calculated by the following equation.

$$\Delta E = \sqrt{(\Delta L)^2 + (\Delta a)^2 + (\Delta b)^2}$$

The negative values of ΔL for the treated stone samples in Table III reflect that the treated stone is less light than the untreated one. Positive values of Δa and Δb indicate that the treated samples are more red and yellow than the untreated one, respectively. However, since the ΔE of the treated stone sample is 2.43 for starch, 2.80 for P(VTMS/12FMA)-*g*-starch and 3.16 for VTMS-starch@p(MMA/BA/3FMA), the color variations induced

Table IV. Capillary Absorption Coefficient, Water Absorption Percent, Water Contact Angle, and Water Vapor Permeability of Treated and Untreated Stone Samples

Protective material	Capillary absorption coefficient/g cm^{-2} s$^{-1/2}$	Water absorption/%	Water contact angle/°	Permeability/g m^{-2}
Starch	6.59×10^{-3}	6.86	undetected	21.1
P(VTMS/12FMA)-*g*-starch	6.90×10^{-3}	6.58	101.7	20.6
VTMS-starch@p(MMA/BA/3FMA)	5.20×10^{-4}	5.80	112.3	19.8
Reference stone	1.19×10^{-2}	9.96	undetected	21.7

Table V. The Weight Loss Percent of the Stones After Salt Crystallization and Freeze-Thaw Cycles

	Salt crystallization cycles		Freeze-thaw cycles	
Protective material	Number	Weight loss/%	Number	Weight loss/%
Starch	S1	31.68	S5	0.36
P(VTMS/12FMA)-*g*-starch	S2	−1.04	S6	0.35
VTMS-starch@p(MMA/BA/3FMA)	S3	−0.44	S7	0.34
Untreated stone	S4	49.95	S8	2.11

Table VI. The Color Variation and Water Static Contact Angles of Protected Stone Specimens After UV Ageing

	P(VTMS/12FMA)-*g*-starch		VTMS-starch@p(MMA/BA/3FMA)	
Ageing time/h	ΔE	θ_w(°)	ΔE	θ_w(°)
0	0.000	102	0.000	112
72	1.096	97	0.958	104
168	1.249	96	1.057	102
336	1.206	95	1.085	100
864	1.473	94	1.623	98
1392	1.974	93	2.050	97

by the applied materials are within acceptable limits when parameter $\Delta E < 5$.

The water capillary absorption reveals the water-resistant property of the different treated stone samples (Figure 6). The given capillary absorption coefficients are evaluated by the slope of initial 10 min of the capillary absorption curves (Table IV). Figure 6 shows the evidence that the untreated stones rapidly absorb a great quantity of water, but this tendency is reduced by every protective treatment. Both P(VTMS/12FMA)-*g*-starch treated stone sample and starch-treated stone sample show much slower absorption speed, the curve of P(VTMS/12FMA)-*g*-starch treated stone sample and starch-treated sample give almost the same capillary absorption coefficient (6.90×10^{-3}–6.59×10^{-3}g cm^{-2} s$^{-1/2}$), and water-absorption percentage (6.58–6.86%) by total immerse (Table IV), much lower than untreated reference stone sample (1.19×10^{-2} g cm^{-2} s$^{-1/2}$, 9.96% water absorption). However, VTMS-starch@p(MMA/BA/3FMA) treated stone sample gains the best water-resistance, because it shows sufficient water-resistant property within 8 h, the lowest water absorption (5.8%) and the lowest capillary absorption coefficient (5.20×10^{-4} g cm^{-2} s$^{-1/2}$). On the other hand, the water contact angles listed in Table IV indicate that the surface of VTMS-starch@p(MMA/BA/3FMA) latex treated stone gains 112.3° as the average value of nine readings, much lower wettability than P(VTMS/12FMA)-*g*-starch treated stone sample (101.7°). The surface of starch-treated stone sample and untreated reference stone samples absorb the water drop immediately during determining so that no water contact angle is detected. Actually, these are corresponding well to the lower water absorption for P(VTMS/12FMA)-*g*-starch and VTMS-starch@p(MMA/BA/3FMA) treated stone samples (6.58 and 5.80%), starch-treated stone sample (6.86%) and untreated stone sample (9.96%) in Table IV.

In order to understand the function of the treated stone sample by fluorosilicone-modified starches, water vapor permeability test of the protected stone is conducted and is listed in Table IV. It is found that the water vapor permeability of protected stone and reference stone are near each other (19.8–21.7g m^{-2}) within 24 h. This could prove that the pores of the sandstone are barely filled by the starches and the protected stone is able

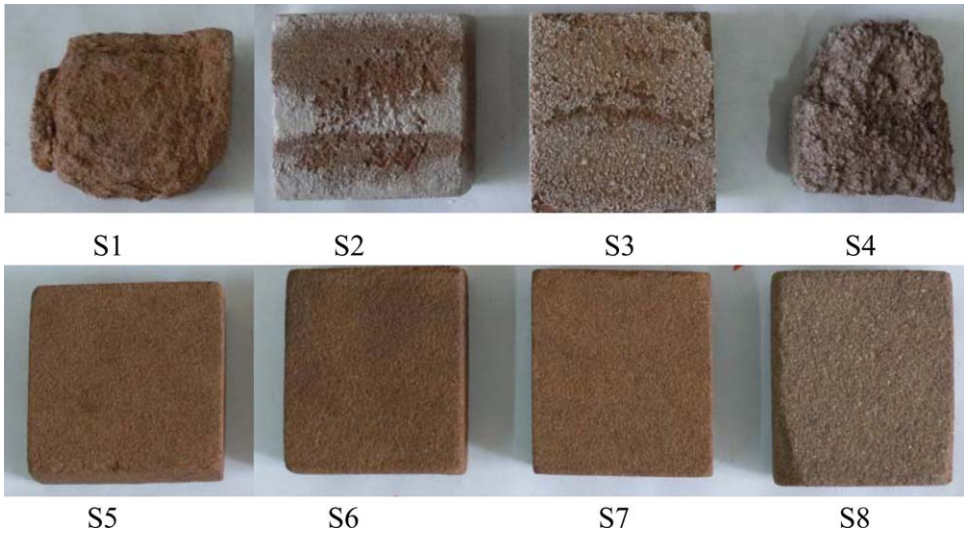

Figure 7. The surface appearance of stone samples after 2 salt crystallization cycles (upper) and 20 freeze-thaw cycles (down). [Color figure can be viewed in the online issue, which is available at wileyonlinelibrary.com.]

to "breath" freely, which is the desired results. Furthermore, the noncontacting surfaces of the treated stone are made wet to test the varying degrees for a few days. The treated-stone by pure starch gets mildewed, while the untreated stone and the stones treated by two fluorosilicone-modified starches are in good condition (not moldy). It indicates that two fluorosilicone-modified starches get obvious resistance against fungus compared to pure starch.

Figure 7 is the surface appearance of stone samples after salt crystallization cycles and freeze-thaw cycles. It is observed that the reference stone (S4) is damaged only one salt crystallization cycle. After two cycles, the starch-treated stone sample is proceeding damaged, but the other two protective stone samples by P(VTMS/12FMA)-*g*-starch (S2) and VTMS-starch@p(MMA/BA/3FMA) (S3) are well preserved after the continuing 10 salt crystallization cycles. The weight loss percents of samples are listed in Table V. The reference and starch-treated stones are damaged seriously with weight loss percent of 31.68 and 49.95%, respectively. P(VTMS/12FMA)-*g*-starch (S2) and VTMS-starch@p(MMA/BA/3FMA) (S4) treated stones show negative values in weight loss due to salt accumulation. It is also possible to observe that VTMS-starch@p(MMA/BA/3FMA) treated stone (S3) is less weathered than P(VTMS/12FMA)-*g*-starch treated stone (S2) from the weight lose, the surface appearance and the salt accumulation. In the freeze-thaw cycles, it is found that some matrix powder in water and some cracks happened in the surface of untreated reference stone sample (S8) at the end of eight cycles with a higher weight loss percent (2.11%), while the other treated stone samples by starch (S5), by P(VTMS/12FMA)-*g*-starch (S6) and by VTMS-starch@p(MMA/BA/3FMA) (S7) remain integrity at the end of 20 cycles (Figure 5) with lower weight loss percents in Table V, indicating a good resistance to freeze-thaw.

In order to imitate a long-time performance of treated stone by fluorosilicone-modified starches, the ultraviolet ageing for the color variation and water static contact angles are shown in Table VI. The color variations of ΔE for the stone specimens are less than two after 1392 h ultraviolet radiation, and the considerable water static contact angles in Table VI also indicate the good resistance of the fluorosilicone-modified starches to ultraviolet radiation.

CONCLUSION

Two fluorosilicone-modified starch materials of P(VTMS/12FMA)-*g*-starch and VTMS-starch@p(MMA/BA/3FMA) are prepared for the protection of historic stones, and their properties and protective performance are evaluated. The grafting fluorosilicone copolymer onto starch improves the uniform aggregate distribution in solution as 40–90 nm for both P(VTMS/12FMA)-*g*-starch and VTMS-starch@P(MMA/BA/3FMA). The surface wettability of films indicates that the water contact angles of films are increased from 51° for starch film into 107° for VTMS-starch@P(MMA/BA/3FMA) film and 72° for P(VTMS/12FMA)-*g*-starch film. Accordingly, the thermal stabilities of both modified starches are also improved for VTMS-starch@p(MMA/BA/3FMA) (320–430°C) and P(VTMS/12FMA)-*g*-starch (320–430°C). After protection, all the chromatic variations are within the acceptable limits. Water-resistance has been improved by every treatment according to water absorption percent. Comparatively, VTMS-starch@P(MMA/BA/3FMA) shows better protective performance in water-resistance by low capillary absorption coefficient (5.2×10^{-4} g cm^{-2} s$^{-1/2}$) and high water contact angle (112.3°). Although both of them reveal prominent salt and freeze-thaw resistance after protection, VTMS-starch@p(MMA/BA/3FMA) shows better performance than P(VTMS/12FMA)-*g*-starch from the weight lose and the weather appearance.

ACKNOWLEDGMENTS

This work has been financially supported by the National Basic Research Program of China (973 Program, No. 2012CB720904), by the National Natural Science Foundation of China (NSFC Grants No. 51073126, 51373133) and by the State Administration of Cultural Heritage (20110128). The authors also wish to express their gratitude for the MOE Key Laboratory for Non-equilibrium Condensed Matter and Quantum Engineering of Xi'an Jiaotong University.

REFERENCES

1. Wei, G. F.; Zhang, H.; Wang, H. M.; Fang, S. Q.; Zhang, B. J.; Yang, F. *Constr. Build. Mater.* **2012**, *28*, 624.
2. Teli, M. D.; Rohera, P.; Sheikh, J.; Singhal, R. *Carbohydr. Polym.* **2009**, *75*, 599.
3. Yang, F.; Zhang, B.; Ma, Q. L. *Acc. Chem. Res.* **2010**, *43*, 936.
4. Carvalho, A. J. F.; Job, A. E.; Alves, N.; Curvelo, A. A. S.; Gandini, A. *Carbohydr. Polym.* **2003**, *53*, 95.
5. Shi, Y. L.; Ju, B. Z.; Zhang, S. F. *Carbohydr. Polym.* **2012**, *88*, 132.
6. Minimol, P. F.; Paul, W.; Sharma, C. P. *Carbohydr. Polym.* **2013**, *95*, 1.
7. Meshram, M. W.; Patil, V. V.; Mhaske, S. T.; Thorat, B. N. *Carbohydr. Polym.* **2009**, *75*, 71.
8. Liang, J. Y.; He, L.; Dong, X.; Zhou, T. *J. Colloid Interface Sci.* **2012**, *369*, 435.
9. Yuan, S.; Pehkonen, S.; Liang, B.; Ting, Y.; Neoh, K.; Kang, E. *Corros. Sci.* **2011**, *53*, 2738.
10. Xiong, D.; Liu, G.; Hong, L.; Duncan, E. *Chem. Mater.* **2011**, *23*, 4357.
11. Kim, N.; Shin, D. H.; Lee, Y. T. *J. Membr. Sci.* **2007**, *300*, 224.
12. Kannarpady, G.; Sharma, R.; Liu, B.; Trigwell, S.; Ryerson, C.; Biris, A. *Appl. Surf. Sci.* **2010**, *256*, 1679.
13. Wang, P.; Schaefer, D. W. *Langmuir* **2008**, *24*, 13496.
14. Loch, C. L.; Ahn, D.; Chen, Z. *J. Phys. Chem. B* **2006**, *110*, 914.
15. Yu, Q.; Xu, J.; Han, Y. *Appl. Surf. Sci.* **2011**, *258*, 1412.
16. Wang, C.; Mao, H.; Wang, C.; Fu, S. *Ind. Eng. Chem. Res.* **2011**, *50*, 11930.

17. Abdelmouleh, M.; Boufi, S.; Salah, A.; Belgacem, M.; Gandini, A. *Langmuir* **2002**, *18*, 3203.
18. Ly, B.; Belgacem, M.; Bras, J.; Salon, M. *Mater. Sci. Eng. C* **2010**, *30*, 343.
19. Mabrouk, A. B.; Salon, M. C. B.; Magnin, A.; Belgacem, M. N.; Boufi, S. *Colloids Surf. A Physicochem. Eng. Aspects* **2014**, *448*, 1.
20. Castellano, M.; Gandini, A.; Fabbri, P.; Belgacem, M. *J. Colloid Interface Sci.* **2004**, *273*, 505.
21. Qu, J.; He, L. *Carbohydr. Polym.* **2013**, *98*, 1056.
22. Yu, Q. J.; Xu, J. M.; Han, Y. Y. *Appl. Surf. Sci.* **2011**, *258*, 1412.
23. Maravelaki-Kalaitzaki, P.; Kallithrakas-Kontos, N.; Agioutantis, Z.; Maurigiannakis, S.; Korakaki, D. *Prog. Org. Coat.* **2008**, *62*, 49.
24. Favaro, M.; Mendichi, R.; Ossola, F.; Russo, U.; Simon, S.; Tomasin, P.; Vigato, P. A. *Polym. Degrad. Stabil.* **2006**, *91*, 3083.
25. Vicini, S.; Mariani, A.; Princi, E.; Bidali, S.; Pincin, S.; Fiori, S.; Pedemonte, E.; Brunetti, A. *Polym. Adv. Technol.* **2005**, *16*, 293.
26. Carretti, E.; Dei, L. *Prog. Org. Coat.* **2004**, *49*, 282.
27. Arienzo, L. D.; Scarfato, P.; Incarnato, L. *J. Cult. Herit.* **2008**, *9*, 253.
28. Sassoni, E.; Franzoni, E.; Pigino, B.; Scherer, G. W.; Naidu, S. *J. Cult. Herit.* **2013**, *14*, e103.
29. Elert, K.; Cultrone, G.; Navarro, C. R.; Pardo, E. S. *J. Cult. Herit.* **2003**, *4*, 91.
30. Zhao, J.; Li, W. D.; Luo, H. J.; Miao, J. M. *J. Cult. Herit.* **2010**, *11*, 279.
31. Toniolo, L.; Poli, T.; Castelvetro, V.; Manariti, A.; Chiantore, O.; Lazzari, M. *J. Cult. Herit.* **2002**, *3*, 309.
32. Kotlik, P.; Doubravová, K.; Horalek, J.; Kubac, L.; Akrman, J. *J. Cult. Herit.* **2014**, *15*, 44.